Journal of Applied Fluid Mechanics, Vol. 12, No. 3, pp. 647-655, 2019.
Available online at www.jafmonline.net, ISSN 1735-3645, EISSN 1735-3645.
DOI: 10.29252/jafm.12.03.28881

Experimental Investigation of Microchannel Heat Sink with Modified Hexagonal Fins

S. Subramanian[1†], K. S. Sridhar[2] and C. K. Umesh[3]

[1]*Microwave Tube Research and Development Centre, BEL, Jalahalli, Bangalore, 560 013 India*
[2]*PES Institute of Technology, 100 feet Ring Road, BSK III Stage, Bangalore, 560 085 India*
[3]*University Visvesvaraya College of Engineering, KR Circle, Bangalore, 560 001 India*

†*Corresponding author Email: subramanian3669@gmail.com*

(Received February 13, 2018; accepted October 23, 2018)

ABSTRACT

The concept of periodic renewal of boundary layers is a promising technique for the enhancement of heat transfer in microchannels. Extending the above concept, microchannel heatsink with modified hexagonal fins has been proposed for disrupting the flow periodically. An experimental study has been carried out to investigate the heat transfer and fluid flow characteristics of a microchannel heat sink with modified hexagonal fins and a conventional type of microchannels with plate fins. The heat transfer and fluid flow characteristics of the modified hexagonal fin microchannels have been compared with the plate fin microchannels. The heat transfer enhancement factor and pressure drop penalty factors are evaluated and compared. The modified hexagonal fin microchannel heat sink has been found to outperform the plate fin microchannel heat sinks in spite of the lesser heat transfer area.

Keywords: Microchannel testing; Modified hexagonal fins; Single phase heat transfer; Copper heat sinks; Laminar flow.

NOMENCLATURE

A	heat transfer area
A_b	area of base excluding fins
A_c	cross sectional area of microchannel
A_{fin}	area of finx
C_c	coefficient of contraction
C_e	coefficient of expansion
D_h	hydraulic diameter
f	friction factor
H	depth of microchannel
h	heat transfer coefficient
K	thermal conductivity
N	number of channel
N_u	Nusselt number
P_r	Prandtl number
ΔP	pressure
ΔP_c	contraction pressure loss
ΔP_e	expansion pressure loss
ΔP_{ch}	channel pressure drop
q	heat load
R_e	Reynolds number
T	temperature of fluid
t	thickness of thermal path
U_{p1}	velocity in the passage at the inlet
U_{p2}	velocity in the passage at the outlet
U	velocity of flow in the channel
W	width
η	fin efficiency
ρ	density of fluid
μ	dynamic viscosity
Subscript	
L	lengthx
L_h	hydrodynamic entry length
Lt	thermal entrance length
out	outlet
in	inlet
smean	average in the solid domain
fmean	average in the fluid domain
s	heating surface
w	wall of microchannel
m	mean
max	maximum
hs	heat sink
ch	channel
f	fluid

1. INTRODUCTION

Microchannels are being explored as a potential option for electronics cooling since Tuckerman *et al.* (1981). The thermal performance of the plate-fin microchannel heatsink decreases in the direction of flow due to the thickening of boundary layer, leading to a wider temperature gradient on the heatsink surface. Hence, there is a continuous demand for the enhancement of heat transfer in the microchannel heatsinks. Various schemes for enhancing the performance of microchannels have been reeported by Steinke *et al.* (2004).

Chen *et al.* (2005) numerically simulated and experimentally tested a heatsink having fractal-tree like microchannels for electronics cooling. Thermal performance was found to improve with the increment of branching levels while leading to an increased manufacturing complexity. Microchannels with wavy walls have been investigated both numerically and experimentally (Gong *et al.*, 2011 & Sui *et al.*, 2010). Microchannels with wavy walls have been reported to enhance the heat transfer up to 26%. Porous honeycomb shaped microchannel system has been tested experimentally by Liu *et al.* (2011). The metallic microchannel heatsink is a potential option for electronics cooling due to its higher thermal performance and structural integrity. Metallic microchannel Heatsink with honeycomb strcuture was found to reach a nearly uniform heat source temperature. Ansari *et al.* (2010) have minimized the thermal resistance of the microchannel with semi-circular grooves at the cost of pumping power. Fin shapes such as circular, square, elliptical and flat with two rounded ends have been simulated numerically by Rubio-Jimenez *et al.* (2012). They have achieved a temperature gradient below 2ºC/mm on the heated wall of the microchannels. Offset fins have been studied by Steinke *et al.* (2006) through analytical and experimental approaches. Tsuzuki *et al.* (2009) have numerically simulated the concept of S-shaped fins for a microchannel heat exchanger with water on one side and sub-critical carbon di-oxide on the other side and they have deduced Nusselt number correlations from the simulated results. Lee *et al.* (2012 and 2013) experimentally tested and numerically simulated oblique shaped fins. The above study concluded that an enhanced heat transfer with a reasonable penalty of pressure is achievable. Though various shapes of fins have been attempted, each design inherited certain drawbacks.

The periodic renewal of boundary layer is a promising technique which has been reported to enhance the heat transfer by Xu *et al.* (2005). Recently heat transfer enhancement using flow disruption techniques have been reviewed comprehensively by Dewan *et al.* (2015). It is reported that flow disruption techniques can enhance the heat transfer effectively. Dewan *et al.* (2017) have analyzed rectangular microchannels with transverse microchambers. The introduction of microchambers in the microchannel path increased the average Nusselt with lower penalty of pressure drop. Chai *et al.* (2018) simulated the effect of five different types of ribs in the microchamber on the thermal hydraulic performance of the microchannels. The thermal resistance of microchannels with ribs is found to decrease from 4 to 31% when compared with the straight fin microchannel heatsink. Convergent-divergent shaped microchannels with or without rib cavities have been simulated by Srivastava *et al.* (2017). The introduction of convergent-divergent ribs and cavities was found to reduce the overall thermal resistance by 40% and make the heatsink surface temperature uniform. A comparative study of microchannels with rectangular shape with and without bifurcation and convergent-divergent shape with and without bifurcation have been simulated by Srivastava *et al.* (2018). It was reported that the convergent-divergent shape with bifurcation transferred the heat better than other geometries. The heat transfer augmentation was attributed to the acceleration of flow, diversion of flow toward the constant cross section segment and periodical interruption and redevelopment of thermal boundary-layers due to bifurcation. From the above literature it is observed that the technique of thermal boundary layer re-development using flow disruption is an effective technique for heat transfer enhancement in microchannel heatsinks.

Heatsinks consisting of fins with the shape of regular hexagons have been tested and optimized with air as the working fluid by Yakut *et al.* (2006). The sizes of the hexagonal fins tested by them were too bigger to be classified as microchannels.

From the above literatures, it is inferred that the modified hexagonal fins are not much explored for enhancing the heat transfer in the microchannels. Hence, a new type of microchannel heatsink has been proposed by modifying the hexagonal shaped fins. The objective of the present work is to study the heat transfer and fluid flow characteristics of a modified hexagonal fin microchannel heatsink through experimentation. The manufacturing method of the heatsink and the experimental test procedures are described. Some of the interesting results are discussed.

2. MODIFIED HEXAGONAL FIN MICROCHANNEL

In the present study, a hexagon with a side length of 500 micrometers have been modified. The included angle of 120º between the sides of a regular hexagon has been modified by restricting the distance between two opposite flat edges of the hexagonal fin to 500 micrometers in one direction. This modification resulted in the acute angles 60º and obtuse angles 150º. The angles were only modified while retaining the length of each side of the hexagonal fins equal to 500 micrometers. When the width of the hexagonal fin is restricted to 500 micrometers in one direction, it appears like a compressed hexagon. This modification has helped in maintaining a common fin thickness between plate fin and hexagonal fin while reducing the size of wake fields behind the fins. Moreover, this modification has led to the formation of divergent and convergent channel at the front and rear ends of the fin which is

beneficial in reducing the pressure drop.

2.1 Dimensional Details of Microchannels

The schematic representations of the modified hexagonal fins arrangement and the plate fin microchannels are shown in Fig. 1 and Fig. 2 respectively. In the plate fin microchannel, the working fluid was pumped from inlet to outlet through the microchannel passages of 500 micrometers width enclosed by the fins of 500 micrometer thickness. In the modified hexagonal fin microchannel heat sink the water was pumped from inlet to outlet through the microchannel passages of 500 microns and the flow got interrupted repeatedly by the in-line fins on the sides.

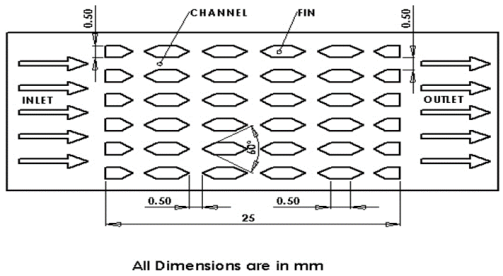

Fig. 1. Sketch of the modified hexagonal fin microchannel heat sink.

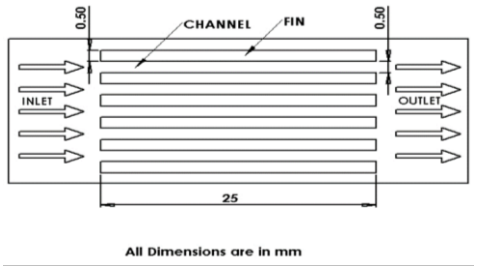

Fig. 2. Sketch of the plate fin microchannel heat sink.

3. Experimental Test Set up

An experimental setup was rigged up to test the fluid flow and heat transfer characteristics of a microchannel heat sink. A schematic diagram of the experimental setup is shown in Fig. 3. The experimental setup consisted of a copper microchannel heat sink, a polycarbonate enclosure to confine the flow through the microchannel heatsink, water reservoir, pump, data acquisition system, power supply, resistance heater, digital Pressure gauge, J type thermocouples, water filter, measuring jar and a stop watch.

The water was sucked from the reservoir through a water filter and pumped to the microchannel heat sink test assembly. The inlet and outlet of the microchannel heat sink test assembly was maintained at the same level to avoid any pressure head variation. The microchannel heat sink was heated by a resistance heater using a power supply. The water absorbed the heat from the microchannels and it was discharged back to the reservoir again. The volumetric discharge of the heated water was measured with the help of a jar and timer. The pressure drop across the microchannel and surface temperatures of the heat sink near the heat source were noted down. The heat transfer coefficient, friction factor and other derived parameters were calculated using the measured data. A picture of the actual arrangement of test set up is shown in Fig. 4.

3.1 Manufacture of Microchannels

Micro end milling process was identified to be the most suited for the fabrication of metallic heat sinks, particularly for the low volume productions (Jasperson *et al.*, 2010). It is a direct method of creating three dimensional shapes predominantly using computer numerically controlled machines. Microchannel heat sinks with 12 rows of modified hexagonal fins and plate fins have been machined out of a copper block on an area of 12.5 mm X 25 mm using CNC micro-milling machine. Microchannels were deburred and polished using diamond coated needle files under a magnification of 3X using a microscope. The center line average values of the surfaces were measured using a surface roughness tester of ZEISS-SURFCOM-130A make. The average roughness of the surface was found to be 1.98 microns. The dimensions were inspected using non-contact video measuring microscope of Micro-Vu-Vertex make. The uncertainty of non contact video measuring machine was 2 micron and the resolution was 0.1 microns.

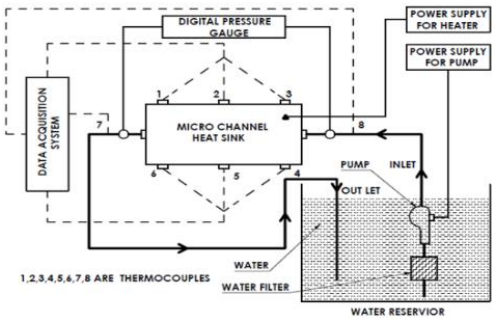

Fig. 3. Schematic diagram of test set up.

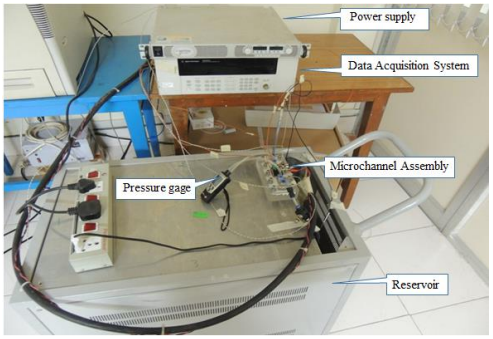

Fig. 4. Picture of actual test set up.

Pictures of a plate fin microchannel heat sink and a modified hexagonal fin microchannel heat sink are shown in Fig. 5. To ensure a common basis for comparison the hydraulic diameters, channel aspect ratios, heat load and mass flow rates were held constant between the two microchannel heatsinks.

The salient features related to the experimental testing are listed in Table 1.

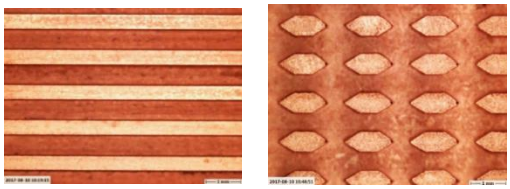

(a) **(b)**

Fig. 5. Microchannels (a) Plate fins (b) Modified hexagonal fins.

Table 1 Salient features related to experimental testing

	Plate fin	Modified hexagonal fin
Width of the channel, μm	570	556
Thickness of the fin, μm	439	448
Depth of the channel, μm	1488	1492
Nominal size of channel, μm	500 X 1500	500 X 1500
Nominal size of fin, μm	500 X 1500	500 on each side X 1500
Length of fin, mm	25.1	24.9
Number of fin rows	12	12
Number of fins per row	1	14
Fin spacing, μm	___	554
Fin length, mm	___	1.327
Length of hexagonal fin side, mm	___	513
Heat transfer area per channel, mm^2	87.5	79.3
Hydraulic diameter, μm	824.3	815
Heat load, W/m^2	$32X10^4$	$32X10^4$
Working fluid	Water	Water
Heatsink material	Copper	Copper
Flow Range, Reynolds number	496 to 1231	552 to 1373

3.2 Comparison of Cost

Since, the cost incurred for overhead and raw materials were the same for both types of microchannels, only machining time was reckoned for the comparison of cost. Machining time of 23 hours were needed for manufacturing the plate fin microchannel heat sink while the modified hexagonal fin microchannel heat sink needed 27 hours of machine time. Thus, the modified hexagonal fin microchannel incurred a machining time of about 17.4 % more than the plate fin microchannels.

3.3 Data Reduction

Hydraulic diameter (Steinke *et al.*, 2006) of the modified hexagonal fin microchannel was calculated from the following equation.

D_h = (4 X Area of free flow X Length of unit cell)/ Area of heat transfer

Area of free flow = width X depth = C X H

Length of unit cell = pitch

From Fig. 6, the heat transfer surface area of the modified hexagonal fin microchannel was determined using the following:

Area of heat transfer = [area of 1-2-3-16

+ area of 8-9-10-11]

+ [area of 4-7-15-12]

+ [area 3-4-5 + area 14-15-16

+ area 10-11-12 + area 6-7-8]

+ [length 3-5-6-8 X depth

+ length 16-14-13-11 X depth]

= [((P-L)/2) X (C+F)] + [C X L] + [4 X 0.5 X (F/2) X ((L-P)/2)] +[6 X S X H]

D_h = 0.000815 m

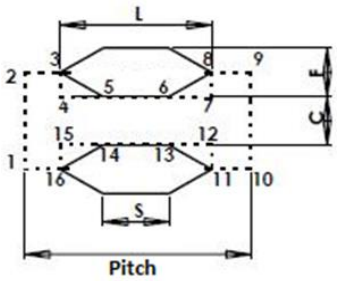

Fig. 6. Unit cell of modified hexagonal fins.

Hydraulic diameter of the plate fin microchannel:

$$D_h = \frac{4 \times \text{Cross sectional area of microchannel}}{\text{Perimeter of the microchannel}} = \frac{2 W_{ch} L_{ch}}{(W_{ch} + L_{ch})}$$

$$= 0.000824 \text{m}$$

The following correlations (Lee *et al.*, 2012) have been used for the derived parameters. The overall heat transfer coefficient (h) was evaluated from the equations below.

$$h = \frac{q}{A(T_{smean} - T_{fmean})} \quad (1)$$

Area of the microchannel $A = A_b + \eta A_{fin}$ (2)

Since the thermal conductivity of the enclosures were considerably lower, the fin tips were treated as adiabatic. The fin efficiency was estimated from the equations below.

$$\eta = \frac{\tanh(mH)}{mH} \quad (3)$$

$$m = \sqrt{\frac{h P}{K_{hs} A_c}} \quad (4)$$

The equations from 1 to 4 were solved iteratively to obtain the heat transfer coefficient. The thermocouples were placed on the surface, where the heat source was mounted. The wall temperature of the microchannel was determined by assuming one dimensional heat conduction.

$$T_w = T_s - \frac{t\,q}{A_c K_{hs}} \tag{5}$$

The Nusselt number was estimated from the following:

$$N_U = \frac{hD_h}{K_f}\,N_U = \frac{hD_h}{K_f}\,N_u = \frac{h\,D_h}{K_f} \tag{6}$$

Minor losses and frictional losses are induced in the fluid flows due to contractions and expansions, when it flows from inlet passage to outlet passage through the microchannels. The pressure drop measurement included the combined losses of the above. The measured pressure drop needed correction (Liu *et al.*, 2004) to determine the actual pressure drop. The following equations (Ansari *et al.*, 2010; Rubio-Jimenez *et al.*, 2012 & Steinke *et al.*, 2006) were used for the calculations of pressure drop.

Pressure drop in the microchannel

$$\Delta P_{ch} = \Delta P - \left(\Delta P_c + \Delta P_e\right) \tag{7}$$

Pressure loss due to sudden contraction

$$\Delta P_c = \frac{1}{2}\rho_f\left(U_{in}^2 - U_{p1}^2\right) + \frac{C_c}{2}\,\rho_f U_{in}^2 \tag{8}$$

Pressure loss due to sudden expansion

$$\Delta P_e = \frac{1}{2}\rho_f\left(U_{p2}^2 - U_{out}^2\right) + \frac{C_e}{2}\,\rho_f U_{out}^2 \tag{9}$$

The friction factor of the measured pressure drop

$$f = \frac{\Delta P_{ch} D_h}{2\,\rho_f\,U_{max}^2 L_{ch}}\;\; f = \frac{\Delta P_{ch} D_h}{2\rho U_{max}^2 L_{ch}}\;\; f = \frac{\Delta P_{ch} D_h}{2\rho U_{max}^2 L_{ch}} \tag{10}$$

3.4 Experimental Uncertainties

During the course of experimentation, the burrs in the heat sink, trapped air bubbles, clogging of dust particles and surface roughness of the connector inner passages were found to affect the measured values to a large extent. These errors were eliminated by careful and repeated inspection at every stage. The uncertainties of measured values have been evaluated with respect to instrument manufacturer's data sheet. The uncertainties associated with experimental test set up have been estimated using the error analysis principles by Taylor (1982). The maximum uncertainty of Nusselt number is found to be below 11.8%. The maximum uncertainty of pressure drop was less than 6%.

3.5 Validation

Heat transfer and fluid flow characteristics of the plate fin microchannels are well established in the literature. Hence, a plate fin microchannel heat sink having a nominal dimensions identical to the modified hexagonal fin microchannel was considered as the basis for the validation of the experimental test procedure.

The developed flow correlations available in the literature are derived for the conditions of the fully developed velocity profile, whereas in the developing region of flow, the velocity profile is not fully developed. Thus, the developed flow correlations are not applicable for the developing region of flow. When a flow consists of both the developing and developed regions, then appropriate correlations which account for both the regions of flow are required to be used.

In view of the above, it was felt necessary to check the state of flow prevailing inside the passage of a microchannel for selecting appropriate correlations. The developing nature of flow can be found by calculating the hydrodynamic and thermal entrance lengths using the criteria of $L_h/(R_eD_h)>0.05$ and $L_t/(R_eD_hP_r)>0.05$, respectively. The plate fin microchannel was found to have both the hydrodynamically developing and developed regions for the Reynolds number up to 609. The flow through the plate fin microchannel was found to be in the developing region for the Reynolds numbers beyond 609. The flow through the plate fin microchannel was found to be in the thermally developing region, for the entire range of Reynolds numbers considered.

Since the flow was found to have both developing region and developed region for the 25mm long plate fin micro channel heat sink, the correlations of Biswal *et al.* (2009) which account for both the developing and the developed regions, have been used for validating the heat transfer and fluid flow characteristics of the plate fin microchannel heat sink. The correlations used for the validation are shown below.

$$\text{Fin effeiciency}, \eta = \frac{\tanh(m\alpha)}{m\alpha} \tag{11}$$

$$\text{Reynolds number}, R_e = \frac{\rho_f\,U_m D_h}{\mu_f} \tag{12}$$

$$m = \sqrt{N_u \frac{1+\alpha}{\alpha\beta}\frac{K_f}{K_{hs}}} \tag{13}$$

Hydraulic diameter and aspect ratios:

$$D_h = \frac{(2W_{ch}L_{ch})}{(W_{ch}+L_{ch})};\; \alpha = \frac{L_{ch}}{W_{ch}};\; \beta = \frac{W_{fin}}{W_{ch}} \tag{14}$$

Mean fluid velocity in the channel:

$$U_m = \frac{V_f}{(NW_{ch}L_{ch})};\; N = \frac{(W_{hs}+W_{fin})}{(W_{ch}+W_{fin})} \tag{15}$$

Poiseuille numbers:

$$f.R_e = \left[\{3.2((R_eD_h)/L_{hs})^{0.57}\}^2 + (4.7+19.64G)^2\right]^{\frac{1}{2}} \tag{16}$$

$$\left(\alpha^{-2}+1\right)/\left(\alpha^{-1}+1\right)^2 \quad (17)$$

$$\sigma = \frac{NW_{ch}}{W_{hs}} \quad (18)$$

Loss coefficient:

$$M = 0.6\,\sigma^2 - 2.4\sigma + 1.8 \quad (19)$$

Pressure drop across the channel:

$$\Delta P = \frac{\rho_f U_{max}^2}{2}\left(4f\,\frac{L_{hs}}{D_h} + M\right) \quad (20)$$

Nusselt number for developing and developed flow:

$$N_u = \left[\left\{2.22\left(R_e P_r D_h / L_{hs}\right)\right\}^{0.33} + \left(8.31G - 0.02\right)^3\right]^{\frac{1}{3}} \quad (21)$$

$$N_u = \left(hD_h\right)/K_f \quad (22)$$

4. Results And Discussions

Figure 7 illustrates the variation of pressure drop across the plate fin microchannel with the Reynolds number of flow through plate fin microchannel. The pressure drop increases with the Reynolds number of the flow, due to the increased frictional losses at higher velocities. The experimental data are found to fall within a mean average error value of 5.2% with the values predicted by the correlations. This deviation is due to the reason that the present correlations do not account for temperature dependent material properties.

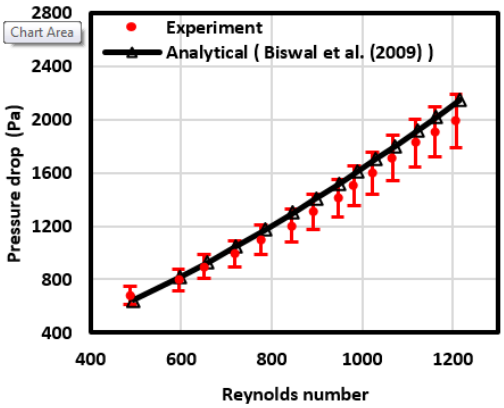

Fig. 7. Variation of pressure drop with the Reynolds number of the plate fin microchannel.

Figure 8 illustrates the variation of heat transfer coefficient with the Reynolds number of the flow through the plate fin microchannel. Reynolds number is a function of inlet flow velocity. The heat transfer coefficient increases with velocity, as the thickness of the thermal boundary layer reduces with increased inlet velocity. The experimental data is quite consistent with the predictions of the correlations, and is found to be within an error value of 1.5%.

Figure 9 compares the variation of pressure drop with Reynolds number for both the plate fin microchannel and modified hexagonal fin microchannel heatsinks. The pressure drop variation of modified hexagonal fin microchannel is higher than the plate fin microchannel. The fin to fin gap acts like a convergent and divergent passage. The flow diverges at the trailing edge of fin which leads to pressure recovery. The pressure builds up as the flow enters the converging passage formed at the leading end of successive fins. As more fluid is forced through the convergent section, boundary layers are re-initialized at the flat edge of the fin. Thinner boundary layers are formed by the faster moving fluids resulting in higher pressure drop. As the Reynolds number increases, higher velocity flow induces strong momentum which further enhances the heat transfer with additional penalty of pressure drop. From the experimental data, the pressure drop of the plate fin microchannel is found to vary from 686 Pa to 1990 Pa while the pressure drop of the modified hexagonal fin microchannel is found to vary from 1025 Pa to 2959 Pa for the same range of Reynolds number.

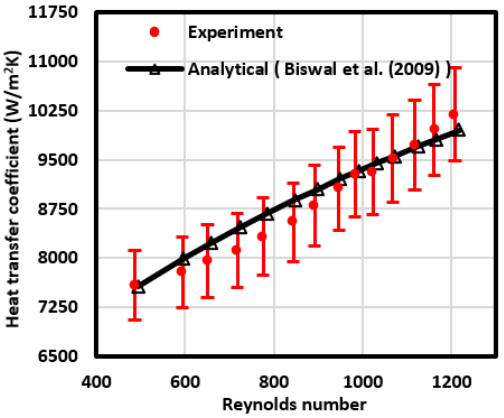

Fig. 8. Variation of heat transfer coefficient with Reynolds number of the plate fin microchannel.

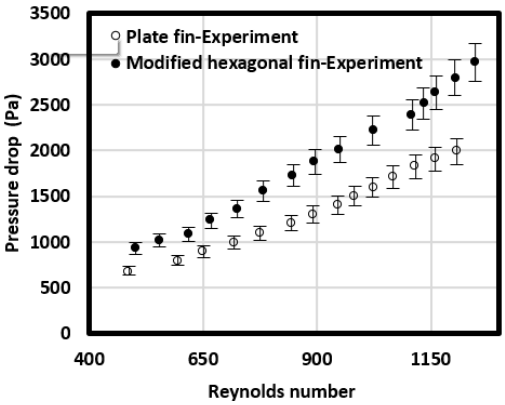

Fig. 9. Comparison of pressure drops incurred in the microchannels.

Figure 10 compares the variation of average Nusselt numbers with Reynolds numbers for both plate fin microchannel and modified hexagonal fin microchannel heatsinks. The average Nusselt number for both configurations increases with

Reynolds number, as the thickness of the thermal boundary layer decreases, due to the increased velocity of flow. Particularly, the heat transferred by the modified hexagonal fin microchannel is significantly higher than the plate fin microchannel. From the experimental data, the average Nusselt number of modified hexagonal is found to be 18.36 at the Reynolds number of 486 which is around 77.3 % more than the plate fin microchannel. This appreciable improvement in average Nusselt number is due to the combined effects of boundary layer redevelopment at the leading edge of each modified hexagonal fin and the fluid mixing between fins. A 112% enhancement in the heat transfer is observed at the Reynolds number of 1207.45, where the average Reynolds number has increased from 18.36 to 29.73. As the Reynolds number increases, stronger momentum is induced by the faster moving fluid leading to an augmented heat transfer with the increased penalty of pressure drop.

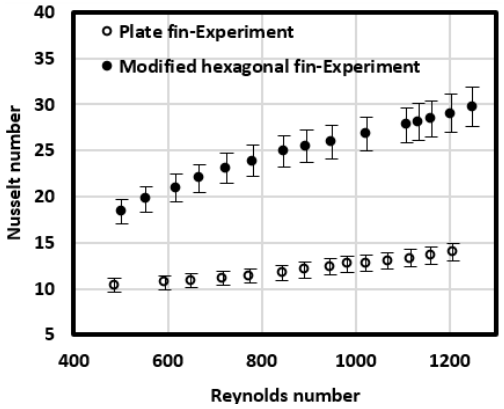

Fig. 10. Comparison of Nusselt number between microchannels.

Figure 11 compares the variation of heat transfer coefficient with the pressure drop across the plate fin microchannel and modified hexagonal fin microchannel. The modified hexagonal fin microchannel is found to incur higher pressure drop than the plate fin microchannels for the same range of Reynolds number of flow. The heat transfer coefficient of modified hexagonal is greater than the plate fin microchannels for any given pressure drop. Pumping power is the product of the pressure drop and volumetric flow rate. Volumetric flow is considered constant, as the inlet velocity of flow and cross sectional area of the microchannel at the inlet are held constant for both the geometries. Modified hexagonal fin microchannel design leads to higher heat transfer coefficient than plate fin microchannel for the same pumping power. Thus, the modified hexagonal fin microchannel is found to excel, due to the advantage of higher heat transfer coefficient per unit pumping power.

Figure 12 compares the experimental data of the variation of maximum wall temperatures of the plate fin and modified hexagonal fin microchannels with Reynolds numbers. Higher heat transfer coefficient, due to strong mixing of fluid in the modified hexagonal fin microchannel, results in a significantly lower temperature of heat sink. The maximum temperature of the heated wall of the microchannel above the inlet temperature of water is 318.2K for the modified hexagonal fin at the Reynolds number of 486 while the maximum temperature above the inlet temperature of water, for the plate fin microchannel is 321.9K. A further reduction in temperature is recorded at higher flow rates in conjugation with increased heat transfer. At the Reynolds number of 1207.45, the modified hexagonal fin microchannel reached a maximum wall temperature rise of 310.4K while the plate fin microchannel recorded a maximum wall temperature of 315.6K at Reynolds number of 1207.45. Due to the introduction of the modified hexagonal fins in the microchannel, the maximum wall temperature is reduced by 5.2K.

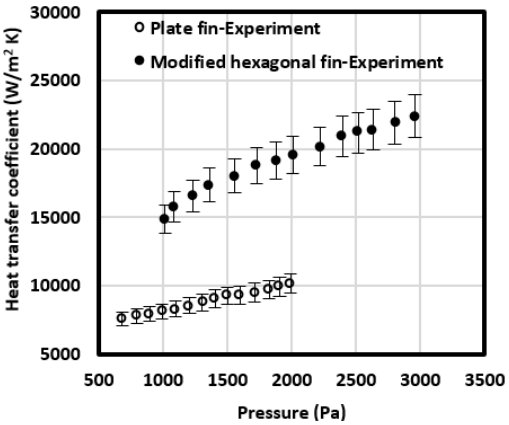

Fig. 11. Variations of heat transfer coefficient with pressure drop.

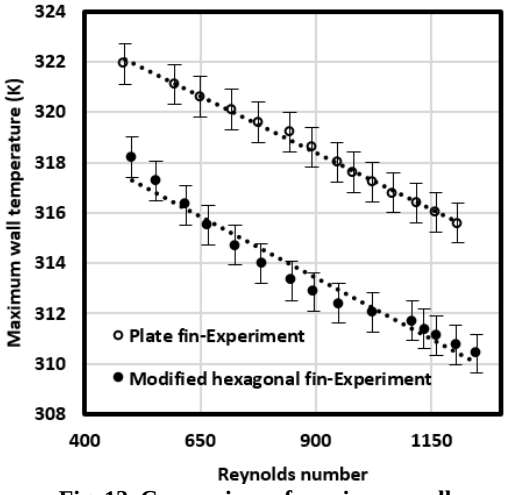

Fig. 12. Comparison of maximum wall temperatures.

Figure 13 compares the performance factors calculated from the experimental data of modified hexagonal fin microchannel with plate fin microchannel. Pressure drop penalty factor and heat transfer enhancement factors are considered as the performance factors for the comparison. The pressure drop penalty factor is defined as the friction factor of the modified hexagonal fin microchannel divided by the friction factor of the plate fin microchannel. The heat transfer enhancement factor

is defined as the average Nusselt number of the modified hexagonal fin microchannel divided by the average Nusselt number of the plate fin microchannel.

It is observed that the pressure drop penalty factor is smaller than the heat transfer enhancement factor. As the Reynolds number increases, the heat transfer enhancement is found to be more than a factor of 2, which means an enhancement of 100%. The pressure drop penalty due to the introduction of the modified hexagonal fins in the microchannel is found to vary from 52 to 72% for the range of Reynolds numbers tested. The benefit of heat transfer enhancement is found to dominate significantly over the pressure drop penalty.

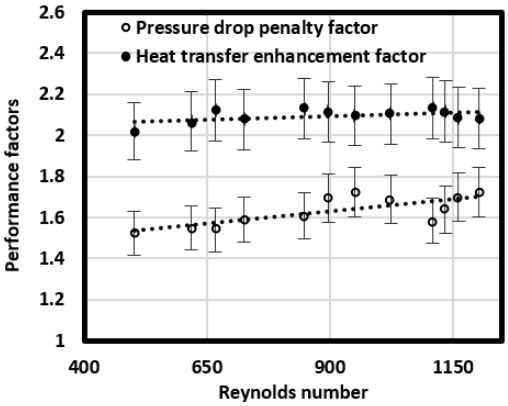

Fig. 13. Comparison of performance factors between the microchannels.

5. CONCLUSION

The machining time of the modified hexagonal fin microchannel heat sink is found to be 17.4 % more than the plate fin microchannel heat sink.

The recurrent re-initialization and thinning of boundary layer ensures that the flow is always in the developing state, thereby contributing for the enhancement of heat transfer.

The pressure drop variation of modified hexagonal fin microchannel is higher than the plate fin microchannel.

Nusselt number of the modified hexagonal fin is found to increase significantly with Reynolds number than the plate fin microchannels.

The maximum wall temperature of the modified hexagonal fin microchannel is found to be lesser by 5.2K than the plate fin microchannel for the test conditions of the present work.

Modified hexagonal fin microchannel design leads to higher heat transfer coefficient than plate fin microchannel for the same pumping power. The benefit of heat transfer enhancement is found to outweigh the penalty of increased pressure drop.

The modified hexagonal fins are performing better than the plate fin microchannels, though the modified hexagonal fin microchannel has 9.4% lesser heat transfer area than the plate fin microchannel.

The experimental testing has proved that the hexagonal fin microchannel heat sink can be considered as a potential option for electronics cooling as the heat transfer enhancement is significant.

ACKNOWLEDGEMENTS

The authors acknowledge Dr Sudhir Kamath, the director, Microwave Tube Research and Development Centre, Bangalore, India for extending technical support for this work.

REFERENCES

Ansari, D., A. Hussain and A. Y. Kim (2010). Multiobjective optimization of a grooved micro-channel heat sink. *IEEE Transactions on Components and Packaging Technology* 33(4), 767-776.

Biswal, L., S. Chakraborthy and S. K. Som (2009). Design and optimization of single-phase liquid cooled microchannel heat sink. *IEEE Transactions on Components and Packaging Technology* 32(4), 876-886.

Chai, L. and L. Wang (2018).Thermal-hydraulic performance of interrupted microchannel heat sinks with different rib geometries in transverse microchambers. *International Journal of Thermal Sciences* 127, 201-212.

Chen, Y. and P. Cheng (2005). Experimental investigation on the thermal efficiency of fractal tree-like microchannel nets. *International Communications on Heat and Mass Transfer* 32, 931-938.

Dewan, A. and H. Kamal (2017). Analysis of interrupted rectangular microchannel heat sink with high aspect ratio. *Journal of Applied Fluid Mechanics* 10, 117-126.

Dewan, A. and P. Srivastava (2015). A review on heat transfer enhancement through flow disruption in a microchannel. *Journal of Thermal Science* 24(3), 203-214.

Gong, L. J., K. Kota, W. Tao and Y. Joshi (2011).Thermal performance of microchannels with wavy walls for electronics cooling. *IEEE Transactions on Components Packaging and Manufacturing Technology* 1(7), 1029-1034.

Jasperson, B. A., Y. Jeon, K. T. Turner, F. E. Pfefferkorn and W. Qu (2010). Comparison of micro-pin-fin and microchannel heat sinks considering thermal-hydraulic performance and manufacturability. *IEEE Transactions on Components and Packaging Technology* 33(1), 148-160.

Lee, P. S. and S. V. Garimella (2005). Hotspot thermal management with flow modulation in a microchannel heatsink. Proceedings of ASME

IMECE: *International Mechanical Engineering Congress & Exposition*, 643-647

Lee, Y. J., P. S. Lee and S. K. Chou (2012). Enhanced thermal transport in microchannel using oblique fins. *Journal of Heat transfer* 134, 101901-1-101901-10.

Lee, Y. J., P. S. Lee and S. K. Chou (2013). Numerical study of fluid flow and heat transfer in the enhanced microchannel with oblique fins. *Journal of Heat transfer* 135, 041901-1-041901-10.

Liu, D. and S. V. Garimella (2004). Investigation of liquid Flow in microchannels. *Journal of Thermophysics and Heat transfer* 18(1), 65-72.

Liu, Y., X. Luo and W. Liu (2011). Experimental research on honeycomb microchannel cooling system. *IEEE Transactions on Components, Packaging and Manufacturing Technology* 1(9), 378-1386.

Rubio-Jimenez, C. A., S. G. Kandlikar and A. H. Guerrero (2012). Numerical analysis of noval micro pin fin heat sink with variable density. *IEEE Transactions on Components, Packaging and Manufacturing Technology* 2(5), 825-833.

Srivastava, P. and A. Dewan (2018). Effect of bifurcation on thermal characteristics of convergent-divergent shaped microchannel. *ASME Journal of Thermal Science and Engineering Applications* 10(4), 041008.

Srivastava, P., A. Dewan and J. K. Bajpai (2017). Flow and heat transfer characteristics in convergent-divergent shaped microchannel with ribs and cavities. *International Journal of Heat and Technology* 35(4), 863-873.

Steinke, M. E. and S. G. Kandlikar (2004). Single phase heat transfer enhancement techniques in the microchannel and minichannel flows. *Proceedings of ASME 2nd International Conference on Microchannels and Minichannels (ICMM 2004)*,Rochester, New York, USA, paper no-228, 141-148.

Steinke, M. E. and S. G. Kandlikar (2006). Single-Phase Liquid Heat Transfer Enhancement in Plain and Enhanced Microchannels. *Proceedings of ASME 4th International Conference on Microchannels and Minichannels*, Limerick,Ireland.

Sui, Y., C. J. Teo, P. S. Lee, Y. T. Chew and C. Shu (2010). Fluid flow and heat transfer in wavy microchannel. *International Journal of Heat and Mass Transfer* 53, 2760-2772.

Taylor, J. R. (1982). *An Introduction to Error analysis*. University Science Books, California.

Tsuzuki, N., M. Utamura and T. Ngo (2009). Nusselt number correlations for a microchannel heat exchanger hot water supplier with S-shaped fins. *Applied Thermal Engineering* 29, 3299-3308.

Tuckerman, D. B. and R. F. W. Pease (1981). High-performance heat sinking for VLSI. *IEEE Electron Device Lett.* EDL-2(5),126–129.

Xu, J. L., Y. H. Gan, D .C. Zhang and X. H. Li (2005) Microscale heat transfer enhancement using thermal boundary layer redevelopment concept. *International Journal of Heat and Mass Transfer* 48,1662-1674.

Yakut, K., N. Alemdaroglu, I. Kotcigolu and C. Celik, (2006). Experimental investigation of thermal resistance of a heat sink with hexagonal fins. *Applied Thermal Engineering* 26, 2262-2271.